Limitations in Spectral Efficiency of a Rate-Adaptive MIMO System Utilizing Pilot-Aided Channel Prediction

Bengt Holter, Geir E. Øien, Kjell J. Hole, and Henrik Holm
Norwegian University of Science and Technology
Department of Telecommunications
O.S.Bragstads plass 2B, N-7491, Trondheim, Norway

***Abstract*— A performance analysis of an adaptive coded modulation (ACM) system operating on a multiple-input multiple-output (MIMO) channel with uncorrelated Rayleigh fading subchannels is presented. Rate adaptation is based on periodically transmitted channel state information (CSI) back to the transmitter, providing information about the channel signal-to-noise ratio (CSNR) *as predicted by the receiver*. Transmit diversity is utilized by employing space-time block coding (STBC) at the transmitter.**

I. Introduction

Adaptive coded modulation (ACM) is a promising data transmission scheme for simultaneously achieving high spectral efficiency and a low bit error rate (BER) on wireless and mobile channels [1]. In [2], a method for assessing performance merits of an ACM system has been employed to evaluate the average spectral efficiency (ASE) of a rate-adaptive coding scheme utilizing any set of multi-dimensional trellis codes originally designed for additive white Gaussian noise (AWGN) channels. The analysis is based on a single-input multiple-output (SIMO) flat-fading channel with statistically independent and identically distributed (i.i.d.) Rayleigh fading subchannels. Perfect coherent detection is assumed and maximum ratio combining (MRC) is employed to maximize the overall received *channel signal-to-noise ratio* (CSNR).

Motivated by the fact that many base stations already are equipped with multiple antennas, the results in [2] are extended to encompass a multiple-input multiple-output (MIMO) flat-fading channel. In a MIMO system, the benefit of transmitting from multiple antennas may be utilized to improve either the diversity order or the information rate of the system. These two transmission strategies are commonly denoted as MIMO diversity and spatial multiplexing, respectively [3]. In this study, a MIMO diversity system is analysed, since it represents a natural extension of the approach in [2]. Transmit diversity is realized by utilizing space-time block coding (STBC) at the transmitter [4], [5].

The rest of this paper is organized as follows. In Section II, the system model is presented. The MIMO channel model is presented in Section III, and in Section IV, formulas to determine the average BER and ASE of a rate-adaptive MIMO diversity system is presented. Simulation results are presented in Section V and conclusions are given in Section VI.

II. System model

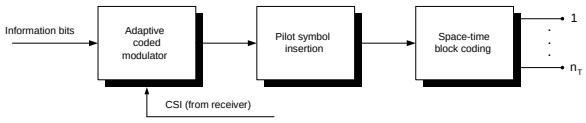


Fig. 1. Transmitter

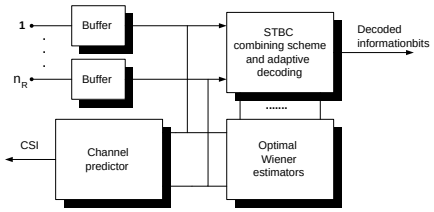


Fig. 2. Receiver

The rate-adaptive MIMO diversity system considered is depicted in Figure 1 (transmitter) and Figure 2 (receiver). The number of transmit and receive antennas is denoted by n_T and n_R, respectively. The adaptive coded modulator/demodulator contains N transmitter-receiver pairs, indexed by $n \in \{1, 2, \ldots, N\}$. Transmitter n has a spectral efficiency of R_n information bits/s/Hz, such that $R_1 < R_2 < \ldots < R_N$, and is designed to provide BER $\leq$ BER$_0$ (a desired target BER) on an AWGN channel with CSNR $\geq \gamma_n$.

The codes are based on quadrature amplitude modulation (QAM) signal constellations with different number of symbols $M_n = 2^{k_n}$, where k_n is some positive integer. Rate adaptation is performed by splitting the CSNR range into $N + 1$ fading regions (bins) and letting the transmitter respond according to the overall (total) CSNR *as predicted by the receiver*. When the predicted CSNR falls within the fading region $[\gamma_n, \gamma_{n+1}\rangle$, the associated channel state information (CSI), i.e. the fading region index n, is sent back to the transmitter. The transmitter then adapts its transmission rate according to the predicted quality of the channel by transmitting with a signal constellation realizing a spectral efficiency of R_n. If the

predicted CSNR falls into the interval $[0, \gamma_1\rangle$, no information is transmitted (outage).

The CSI is assumed conveyed to the transmitter through a zero-error feedback channel, but by the time the CSI is received by the transmitter, it may deviate from the *true* channel state due to a non-zero return channel time-delay τ. As a result, the transmitter may transmit at either a too low or too high information rate, affecting the average BER, ASE, and outage probability of the system. The time-delay τ consists of a sum of the processing time used for CSNR prediction, transmission protocol delays, physical feedback transmission time, and time used for transmitter reconfiguration [2]. Other factors making an impact on the system performance are the temporal fading correlation, the average channel quality, the number of codes/signal constellations, and how the CSNR is predicted.

For comparison reasons, all simulation results presented in section V are based on the same assumptions as in [2] regarding the temporal fading correlation (Jakes spectrum) and the number of codes/signal constellations. A channel predictor optimal in the *maximum a posteriori* sense is utilized, and the CSI estimation is assumed done by an optimal non-causal Wiener interpolator filter, allowing true coherent detection to be assumed.

III. Channel model

In this section, the MIMO channel model is presented. In order to relate the results obtained in this study with the results presented in [2], the SIMO channel model and some important CSNR statistic results obtained in [2] are reviewed in the first subsection.

A. SIMO channel model

A flat-fading SIMO system with n_R receive antennas and MRC at the receiver is considered. The complex baseband representation of the received signal at each of the receiving antennas can be expressed as $\mathbf{x} = \mathbf{h}s + \mathbf{n}$, where $\mathbf{x} \in \mathbb{C}^{n_R}$ denotes the vector of received signals per channel use, s denote the transmit symbol, $\mathbf{h} \in \mathbb{C}^{n_R}$ denote the SIMO channel vector, and $\mathbf{n} \in \mathbb{C}^{n_R}$ denotes the AWGN vector, where each entry of the vector is a zero-mean, complex Gaussian random variable with equal variance σ_n^2.

The MRC output is a linear combination of the branch signals, and the overall received CSNR per symbol may be expressed as [6]

$$\gamma = \frac{P_T ||\mathbf{h}||_2^2}{\sigma_n^2}, \tag{1}$$

where P_T denotes the constant average transmit power and $||\cdot||_2^2$ denotes the squared Euclidean norm. From (1), the statistics of γ is governed by the statistics of $||\mathbf{h}||_2^2$. The envelopes of the entries in the channel vector $\mathbf{h}$ are modelled as i.i.d. Rayleigh random variables. From this assumption, it can be shown that the overall CSNR γ will follow a Gamma distribution $\mathcal{G}(\alpha, \beta)$ with shape parameter $\alpha = n_R$ and scale factor $\beta = \overline{\gamma}_l$, where $\overline{\gamma}_l$ denotes the average CSNR received on any channel l.

Note that due to the i.i.d. assumption of the channels, the average CSNR on all channels will be equal. However, the average CSNR per channel $\overline{\gamma}_l$ will still be indexed by l in order to indicate that this is not the overall expected CSNR γ. Also due to the independence assumption of the subchannels, the *predicted* overall CSNR $\widehat{\gamma}$ may be expressed as a Gamma distributed random variable $\widehat{\gamma} \sim \mathcal{G}(n_R, r\overline{\gamma}_l)$, where the parameter r is the ratio between the expectation of the predicted and the true CSNR.

B. MIMO channel model

In a flat-fading MIMO diversity system, the complex baseband representation of the input/output relations can be expressed as $\mathbf{x} = \mathbf{H}\mathbf{s} + \mathbf{n}$, where $\mathbf{x} \in \mathbb{C}^{n_R}$ denotes the vector of received signals per channel use, $\mathbf{s} \in \mathbb{C}^{n_T}$ denotes the vector of transmit symbols, $\mathbf{H} \in \mathbb{C}^{n_R \times n_T}$ denotes the MIMO channel matrix, and $\mathbf{n} \in \mathbb{C}^{n_R}$ denotes the AWGN vector, where each entry of the vector is a zero-mean, complex Gaussian random variable with equal variance σ_n^2. The complex entry h_{ij} of the channel matrix $\mathbf{H}$ denotes a flat-fading channel between transmit antenna j and receive antenna i. It will be assumed that all envelopes in $\mathbf{H}$ are i.i.d. Rayleigh random variables.

Using STBC at the transmitter, the total received CSNR per symbol may be written as [7]

$$\gamma = \frac{P_T ||\mathbf{H}||_F^2}{\sigma_n^2 n_T}, \tag{2}$$

where $||\cdot||_F^2$ denotes the squared Frobenius norm. From (2), the statistics of γ is governed by the statistics of $||\mathbf{H}||_F^2$. Using a transformation of random variables it can be shown that γ is a Gamma distributed random variable $\gamma \sim \mathcal{G}(\kappa, \frac{\overline{\gamma}_l}{n_T})$, where $\kappa = n_T \cdot n_R$. As for the SIMO system, the predicted CSNR may also be expressed as a Gamma distributed random variable $\widehat{\gamma} \sim \mathcal{G}(\kappa, \frac{r\overline{\gamma}_l}{n_T})$.

It can be seen that the CSNR analysis of the SIMO system and the MIMO diversity system analysed in this subsection is very similar. Thus, by inserting the new CSNR statistics obtained in this section, the results in [2] may be extended to a MIMO diversity system using the same analysis approach.

IV. BER and ASE analysis

The BER (averaged over all codes and all CSNRs) is given as the average number of bits in error, divided by the average number of bits transmitted [2]

$$\overline{\text{BER}} = \frac{\sum_{n=1}^{N} R_n \cdot \overline{\text{BER}}_n}{\sum_{n=1}^{N} R_n P_n}, \tag{3}$$

where R_n is the information rate of code n, P_n is the probability that code n will be used, and $\overline{\text{BER}}_n$ is the average BER experienced when code n is applied. This may be written as [8]

$$\overline{\text{BER}}_n = \int_{\gamma_n}^{\gamma_{n+1}} \int_0^{\infty} \text{BER}_n(\gamma, \widehat{\gamma}) f_{\gamma,\widehat{\gamma}}(\gamma, \widehat{\gamma}) d\gamma d\widehat{\gamma}, \tag{4}$$

where $\mathrm{BER}_n(\gamma,\widehat{\gamma})$ is the BER experienced when code n is applied, and $f_{\gamma,\widehat{\gamma}}(\gamma,\widehat{\gamma})$ is the joint distribution of the predicted and true CSNR. Since both the true and the predicted CSNR can be modelled as Gamma distributed random variables, $f_{\gamma,\widehat{\gamma}}(\gamma,\widehat{\gamma})$ is a bivariate Gamma distribution.

When code n is operating on an AWGN channel with CSNR γ, the BER-CSNR relationship for varying γ may be approximated by the expression [1]

$$\mathrm{BER} \approx a_n \cdot e^{-\frac{b_n\gamma}{M_n}}, \tag{5}$$

where a_n and b_n are code-dependent constants found by least-square curve fitting to simulated BER-CSNR data on AWGN channels. This approximation is accurate for any CSNR resulting in BER $\lesssim 10^{-1}$ [9]. However, the approximation approaches a_n for low CSNRs, and since a_n can be larger than one [1], the following approximate BER expression for code n is utilized [2]

$$\mathrm{BER}_n(\gamma,\widehat{\gamma}) \cong \begin{cases} a_n \cdot e^{-\frac{b_n\gamma}{M_n}} & \text{when } \gamma \geq \gamma_n^l \\ \frac{1}{2} & \text{when } \gamma \leq \gamma_n^l \end{cases} \tag{6}$$

The boundary $\gamma_n^l = \ln(2a_n)M_n/b_n$ is the smallest CSNR such that the BER is no larger than 0.5 for either code in the set. The boundary is obtained by assuming equality in (5), setting BER $= 0.5$, and solving for γ. Note that the function in (5) is invertible, so the smallest CSNR required to achieve a given target BER, denoted BER_0, can be found. Inserting (6) into (4), the average BER when trellis code n is employed may be expressed as a sum of three separate integrals [2],

$$\begin{aligned} \overline{\mathrm{BER}}_n &= \int_{\gamma_n}^{\gamma_{n+1}} \{\mathcal{J}1(n,\widehat{\gamma}) - (\mathcal{J}21(n,\widehat{\gamma}) - \mathcal{J}22(n,\widehat{\gamma}))\}d\widehat{\gamma} \\ &= \mathcal{I}1(n) - (\mathcal{I}21(n) - \mathcal{I}22(n)), \end{aligned} \tag{7}$$

where

$$\mathcal{J}1(n,\widehat{\gamma}) = \int_0^{\infty} a_n \exp\left(-\frac{b_n\gamma}{M_n}\right) f_{\gamma,\widehat{\gamma}}(\gamma,\widehat{\gamma})d\gamma \tag{8}$$

$$\mathcal{J}21(n,\widehat{\gamma}) = \int_0^{\gamma_n^l} a_n \exp\left(-\frac{b_n\gamma}{M_n}\right) f_{\gamma,\widehat{\gamma}}(\gamma,\widehat{\gamma})d\gamma \tag{9}$$

$$\mathcal{J}22(n,\hat{\gamma}) = \frac{1}{2}\int_0^{\gamma_n^l} f_{\gamma,\widehat{\gamma}}(\gamma,\widehat{\gamma})d\gamma. \tag{10}$$

Using the CSNR statistics for a MIMO diversity system presented in subsection IIIB, the bivariate Gamma distribution may be written as

$$\begin{aligned} f_{\gamma,\widehat{\gamma}}(\gamma,\widehat{\gamma}) &= \frac{(\gamma\widehat{\gamma})^{(\kappa-1)/2}}{\Gamma(\kappa)\left[r\left(\frac{\overline{\gamma}_l}{n_T}\right)^2\right]^{(\kappa+1)/2}(1-\rho)\cdot\rho^{(\kappa-1)/2}} \\ &\times e^{-\frac{\gamma}{\frac{\overline{\gamma}_l}{n_T}(1-\rho)}} \cdot e^{-\frac{\widehat{\gamma}}{\frac{\overline{\gamma}_l}{n_T}(1-\rho)}} \\ &\times \mathrm{I}_{\kappa-1}\left(\frac{2\sqrt{\rho}}{1-\rho}\sqrt{\frac{\gamma\widehat{\gamma}}{r\left(\frac{\overline{\gamma}_l}{n_T}\right)^2}}\right), \end{aligned} \tag{11}$$

where ρ is the normalized power correlation coefficient between the true and predicted CSNR, and $\mathrm{I}_{\kappa-1}(\cdot)$ is the modified Bessel function of the first kind and order $\kappa-1$. The following closed-form expressions for $\mathcal{I}1(n)$, $\mathcal{I}21(n)$, and $\mathcal{I}22(n)$ in (7) are obtained:

$$\begin{aligned} \mathcal{I}1(n) &= a_n\left(\frac{n_T}{\frac{b_n\overline{\gamma}_l}{M_n}+n_T}\right)^{\kappa} \\ &\times \left[Q\left(\kappa, \frac{\gamma_n}{\overline{\gamma}_l r}\cdot\frac{n_T\left(\frac{b_n\overline{\gamma}_l}{M_n}+n_T\right)}{(1-\rho)\frac{b_n\overline{\gamma}_l}{M_n}+n_T}\right)\right. \\ &- \left. Q\left(\kappa, \frac{\gamma_{n+1}}{\overline{\gamma}_l r}\cdot\frac{n_T\left(\frac{b_n\overline{\gamma}_l}{M_n}+n_T\right)}{(1-\rho)\frac{b_n\overline{\gamma}_l}{M_n}+n_T}\right)\right] \end{aligned} \tag{12}$$

$$\begin{aligned} \mathcal{I}21(n) &= a_n\sum_{k=0}^{\infty}\frac{\Gamma(k+\kappa)}{\Gamma(k+1)\Gamma(\kappa)}\left(\frac{\rho}{1-\rho}\right)^k \\ &\times \left(\frac{n_T}{\frac{b_n\overline{\gamma}_l}{M_n}+\frac{n_T}{(1-\rho)}}\right)^{k+\kappa} \\ &\times \left[1-Q\left(k+\kappa, \gamma_n^l\left(\frac{b_n}{M_n}+\frac{n_T}{(1-\rho)\overline{\gamma}_l}\right)\right)\right] \\ &\times \left[Q\left(k+\kappa, \frac{n_T\gamma_n}{(1-\rho)\overline{\gamma}_l r}\right)\right. \\ &- \left. Q\left(k+\kappa, \frac{n_T\gamma_{n+1}}{(1-\rho)\overline{\gamma}_l r}\right)\right] \end{aligned} \tag{13}$$

$$\begin{aligned} \mathcal{I}22(n) &= \frac{1}{2}\sum_{k=0}^{\infty}\frac{\Gamma(k+\kappa)}{\Gamma(k+1)\Gamma(\kappa)}\rho^k(1-\rho)^{\kappa} \\ &\times \left[1-Q\left(k+\kappa, \frac{n_T\gamma_n^l}{(1-\rho)\overline{\gamma}_l}\right)\right] \\ &\times \left[Q\left(k+\kappa, \frac{n_T\gamma_n}{(1-\rho)\overline{\gamma}_l r}\right)\right. \\ &- \left. Q\left(k+\kappa, \frac{n_T\gamma_{n+1}}{(1-\rho)\overline{\gamma}_l r}\right)\right] \end{aligned} \tag{14}$$

With $n_T = 1$ ($\kappa = n_R$), all closed-form expressions are reduced to the SIMO expressions in [2]. For a $2G$-dimensional ($2G$-D) trellis code utilized in [2], where $G \in \{1,2,\ldots\}$, the information rate R_n is obtained as follows. The encoder for code n accepts $p = G\cdot\log_2(M_n) - 1$ information bits at each time index $G\cdot T_s$, where T_s denote the time between transmission of two consecutive QAM modulation symbols. The encoder generates $p+1 = G\cdot\log_2(M_n)$ coded bits which specify G QAM modulation symbols from the nth QAM constellation with $M_n = 2^{k_n}$ symbols. Thus, p information bits are transmitted within $G\cdot T_s$ uses of the channel. The information rate for code n, in information bits per channel use, is then $R_n = \frac{p/(GT_s)}{B}$, where B is the signaling bandwidth. Assuming ideal Nyquist pulses, $B = 1/T_s$, the spectral efficiency of code n is $R_n = k_n - 1/G$ measured in bits/s/Hz.

Using pilot-aided channel prediction, every Lth channel symbol is a pilot symbol and thus does not convey information. The information rate of code n can then be expressed as

$R_n = (k_n - 1/G) \cdot \frac{L-1}{L}$. When pilot-aided channel prediction is utilized in a MIMO diversity system with n_T transmit antennas, n_T times as many pilot symbols are needed as in the SIMO case [4]. It is assumed that when a pilot symbol enters the space-time encoder, it is cyclically shifted and transmitted only once from each transmit antenna within n_T time periods. The data symbols that follows are encoded according to the rules of the chosen STBC.

In this study, the space-time encoder maps K input QAM symbols into n_T orthogonal sequences of length T, where $T = (K/R_s)T_s$, and R_s is the code rate of the employed STBC. Table I summarizes the characteristics of some orthogonal STBC originally derived in [5] for 2, 3, and 4 transmit antennas [10]. Since the different orthogonal designs accept

TABLE I
ORTHOGONAL DESIGNS FOR STBC

Orthogonal design	n_T	R_s	K	T
G_2	2	1	2	2
G_3	3	1/2	4	8
G_4	4	1/2	4	8
H_3	3	3/4	3	4
H_4	4	3/4	3	4

different number of input symbols, the following rules of pilot symbol spacing are assumed:

$$L = \begin{cases} m \cdot n_T + 1 & \text{for } G_2, G_4, H_3 \\ m \cdot 4 + 1 & \text{for } G_3 \\ m \cdot 3 + 1 & \text{for } H_4 \end{cases}, \qquad (15)$$

where $m \in \mathbb{Z}^+, m \neq 0$.

Employing either of the space time codes presented in Table I, the pilot symbol spacing *on a single antenna branch*, L_b, can be written as $L_b = (1/R_s)m \cdot n_T + n_T$. The new pilot spacing L_b can be expressed in terms of the original pilot spacing L as $L_b = (L-1)/R_s + n_T$.

Using the assumptions on pilot spacing in (15), the spectral efficiency of code n in a MIMO diversity system, denoted R_n^{STBC}, can be expressed as

$$\begin{aligned} R_n^{STBC} &= (k_n - 1/G) \cdot \frac{(L_b - n_T)R_s}{L_b} \\ &= (k_n - 1/G) \cdot \frac{(L-1) \cdot R_s}{L - 1 + n_T R_s}. \end{aligned} \qquad (16)$$

The ASE is the average of the information rates R_n^{STBC} for the individual codes [2]

$$\text{ASE} = \sum_{n=1}^{N} R_n^{STBC} \cdot P_n, \qquad (17)$$

where the probability P_n is simply the probability that the predicted CSNR falls into the interval $[\gamma_n, \gamma_{n+1} >$, i.e. $P_n = \int_{\gamma_n}^{\gamma_{n+1}} f_{\widehat{\gamma}}(\widehat{\gamma}) d\widehat{\gamma}$. The predicted overall CSNR $\widehat{\gamma}$ is - as is the actual overall CSNR - a Gamma distributed random variable. The probability P_n can be identified as

$$P_n = Q\left(\kappa, \frac{\gamma_n n_T}{r\overline{\gamma}_l}\right) - Q\left(\kappa, \frac{\gamma_{n+1} n_T}{r\overline{\gamma}_l}\right), \qquad (18)$$

where $Q(x, y)$ is the normalized incomplete gamma function. The ASE for a MIMO diversity system utilizing pilot-aided channel prediction can then be written as

$$\begin{aligned} \text{ASE} &= \sum_{n=1}^{N} (\log_2(M_n) - 1/G) \cdot \left(\frac{(L-1) \cdot R_s}{L - 1 + n_T R_s}\right) \\ &\times \left[Q\left(\kappa, \frac{\gamma_n n_T}{r\overline{\gamma}_l}\right) - Q\left(\kappa, \frac{\gamma_{n+1} n_T}{r\overline{\gamma}_l}\right)\right]. \end{aligned} \qquad (19)$$

Due to an increased number of pilot symbols and the fact that for $n_T > 2$, the code-rate $R_s < 1$ for complex signal constellations [5], the ASE of the MIMO diversity system is upper bounded for a given L by the ASE of the SIMO system in [2]. In the next section, all the closed-form formulas derived in this section are utilized to obtain simulation results on BER and ASE performance of a rate-adaptive MIMO diversity system.

V. SIMULATION RESULTS

For all the results presented in this section, the channel is assumed to be quasi-static, i.e. the fading amplitudes of the channel matrix $\mathbf{H}$ are assumed to be constant between two successive pilot symbols. A rate-adaptive codec with eight 4-dimensional trellis codes is utilized, and for a target $\text{BER}_0 = 10^{-4}$, the parameters a_n and b_n along with the threshold values γ_n^l are the same as presented in Table 3.1 in [2]. Parameters not directly tied to the codes, albeit dependent on the implementation are the carrier frequency $f_c = 2$ GHz, a bandwidth of $B = 400$ kHz, and a terminal velocity of $v = 30$ m/s.

In Figure 3, 4, and 5, the BER as a function of feedback delay and of expected subchannel CSNR for a 1x4, 2x2, and a 3x3 system is presented. The contour lines identify the target $\text{BER}_0 = 10^{-4}$, and the operation of the system is acceptable whenever $\text{BER} \leq \text{BER}_0$. It can be seen that due to the increased stability (diversity order) of the 3x3 system, the BER performance is acceptable within a greater range of CSNRs and delays than the 1x4 and the 2x2 system. The acceptable range for the 1x4 and the 2x2 system is very similar due to the systems having the same diversity order. The price paid for the 2x2 and the 3x3 system is the reduction in ASE. In Figure 6, the relative differences in ASE between a 1x4, 2x2, and 3x3 system is depicted.

VI. CONCLUSIONS

The performance results of a rate-adaptive SIMO system in [2] have been extended to encompass a MIMO diversity system, utilizing STBC at the transmitter. Even though the benefit of having multiple antennas can be utilized to increase the overall diversity order and thus the robustness of BER performance of the system, the increased number of pilot symbols needed to perform channel estimation and prediction reduces the attainable average spectral efficiency of the system. Clearly, in order to take full advantage of the combined capacity potential of MIMO subchannels and ACM, another prediction technique is needed. Decision-directed (DD) estimation or a DD/pilot-aided hybrid may be a candidate.

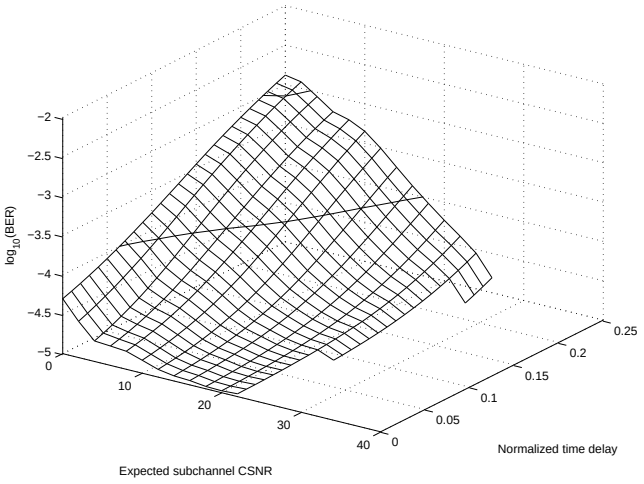


Fig. 3. BER as a function of feedback delay and of expected subchannel CSNR. $\kappa = 5$ antennas are utilized (1×4 system) and the pilot symbol spacing is $L = 7$. The prediction filter length is 1000 taps.

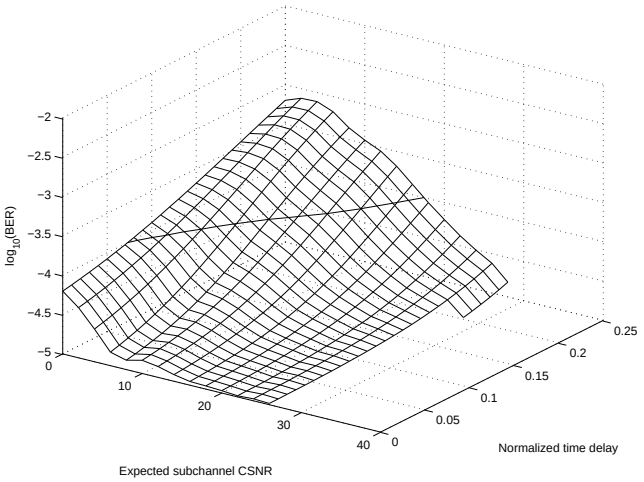


Fig. 4. BER as a function of feedback delay and of expected subchannel CSNR. $\kappa = 4$ antennas are utilized (2×2 system with STBC G_2) and the pilot symbol spacing is $L = 7$. The prediction filter length is 1000 taps.

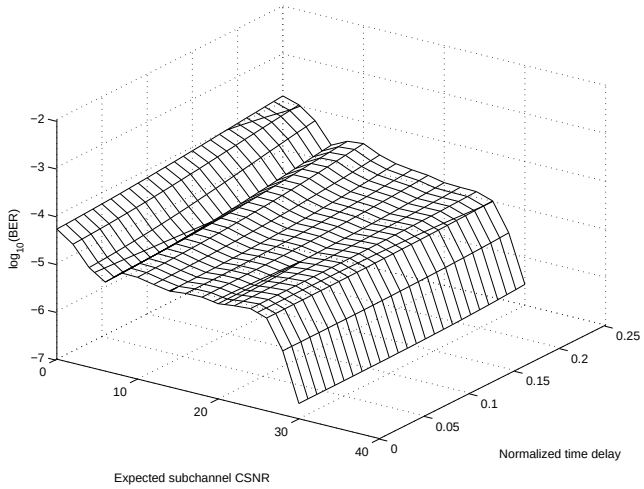


Fig. 5. BER as a function of feedback delay and of expected subchannel CSNR. $\kappa = 6$ antennas are utilized (3×3 system with STBC H_3) and the pilot symbol spacing is $L = 7$. The prediction filter length is 1000 taps.

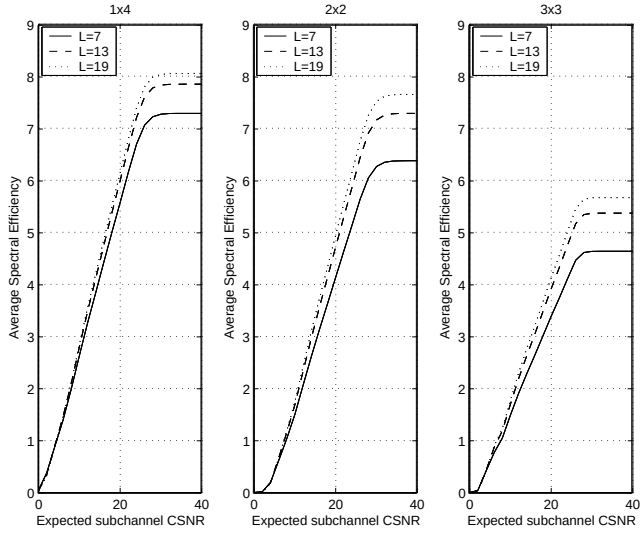


Fig. 6. Average spectral efficiency as a function of expected subchannel CSNR [dB], plotted for various L, for a normalized feedback time delay (symbol duration normalized with respect to maximum Doppler spread) of 0.25.

REFERENCES

[1] K. J. Hole, H. Holm, G. E. Øien, "Adaptive multidimensional coded modulation on flat fading channels," *IEEE J. Select. Areas Commun.*, No. 7, pp. 1153–1158, July 2000.

[2] H. Holm, *Adaptive Coded Modulation and Channel Estimation Tools for Flat Fading Channels*, Ph.D. thesis, The Norwegian University of Science and Technology, April 2002.

[3] R. W. Heath, *Space-Time Signaling in Multi-Antenna Systems*, Ph.D. thesis, Stanford University, November 2001.

[4] S. M. Alamouti, "A simple transmit diversity technique for wireless communications," *IEEE Journal on Selected Areas in Communications*, No. 8, October 1998.

[5] V. Tarokh, H. Jafarkhani, A. R. Calderbank, "Space-time block codes from orthogonal designs," *IEEE Transactions on Information Theory*, No. 5, July 1999.

[6] B. Holter, G. E. Øien, "The optimal weights of a maximum ratio combiner using an eigenfilter approach," *in Proc. 5th IEEE Nordic Signal Processing Symposium (NORSIG-2002), Hurtigruten, Norway*, October 2002.

[7] S. Sandhu, A. Paulraj, "Space-time block codes: a capacity perspective," *IEEE Communications Letters*, No. 12, December 2000.

[8] M. -S. Alouini, A. Goldsmith, "Adaptive modulation over Nakagami fading channels," *Wireless Personal Communications*, pp. 119–143, 2000.

[9] K. J. Hole, H. Holm, G. E. Øien, "Performance analysis of adaptive coded modulation with antenna diversity and feedback delay," *Telektronikk*, No. 1, pp. 106–113, 2002.

[10] R. Gozali, B. D. Woerner, "On the robustness of space-time block codes to spatial correlation," *IEEE Vehicular Technology Conference*, pp. 832–836, 2002.